ChemBioChem

Research Article
doi.org/10.1002/cbic.202400536

Chemistry Europe
European Chemical Societies Publishing

www.chembiochem.org

Modulating Polymerase Activity Through Light-Oxygen-Voltage Domain Insertion

Daniel Hafki,[a] Jonas Alda,[a] Daniel Pietrus,[a] and Susanne Brakmann*[a]

Biochemical reaction networks adapt to environmental conditions by sensing chemical or physical stimuli and using tightly controlled mechanisms. While most signals come from molecules, many cells can also sense and respond to light. Among the biomolecular structures that enable light sensing, we selected a light-oxygen-voltage (LOV) domain in a previous study that tested the engineering of novel regulatory mechanisms into a nucleic acid polymerase. In this follow-up study, we studied the activities of previously selected variants in kinetic detail, and we generated additional LOV-polymerase fusion variants based on further insertion criteria. Our results provide mechanistic insights into how LOV domain insertion influences polymerase activity in a light-responsive manner: All active and photoresponsive enzyme variants studied by us to date were partially inhibited (i.e., "turned off") after irradiation with blue light at 470 nm, which can be explained by specific obstructions of the polymerase entry or exit structures (substrate entry channels or product exit channels, or both). Although the effects observed are moderate, we anticipate further engineering strategies that could be used to improve the extent of switchability and possibly to develop a "turn-on mode" insertion.

Introduction

Chemical and biochemical reactions in living organisms depend on the availability of cellular resources. A variety of different regulatory mechanisms are involved in the necessary adjustments, including the control of reactions and reaction cascades by small molecules, protein-protein interactions, (de)phosphorylation, pH or oxygen, as well as the influence of physical factors such as light or voltage. Light as a signal is of particular interest in current enzyme engineering approaches because it is orthogonal to the aforementioned molecule-based regulatory mechanisms, can be applied precisely in space and time, does not require the use of potentially toxic compounds, is minimally invasive, and reversible. The natural world contains a number of photoresponsive protein domains that absorb light across the visible spectrum.[1] These have become of interest for chemical-biological and especially optogenetic approaches to elucidate complex cellular processes by targeted perturbation of the molecular system combined with differential analysis of the perturbed and unperturbed states.[2]

In this regard, light-oxygen-voltage (LOV)-sensitive domains that can be fused to an effector protein are of particular interest because they are relatively small (144 amino acids; for the complete sequence, see SI) and, via their cofactor flavin mononucleotide (FMN), are stimulated by blue light ($\lambda_{ex,max}$: 450 nm). Light induces the formation of a thioether bond between the flavin and a conserved cysteine residue, triggering rearrangements of the entire LOV domain and ultimately modulating effector activity.[3] In nature, LOV domains are found terminally fused to the effector proteins and, with few exceptions,[4] transduce a signal from an N-terminal photosensory domain to a C-terminal effector domain or protein.[1b] However, this design concept is not applicable to the engineering of all proteins of interest, as terminal amino acids and domains are often involved in (catalytic) activity.

In a previous study,[5] we have addressed this problem by inserting the LOV2 domain from oat (*Avena sativa*) into so-called split positions of bacteriophage T7 RNA polymerase (T7 RNAP).[2a,5–6] This enzyme is of interest for a number of chemical-biological studies due to its efficiency in heterologous expression of recombinant proteins and the large scale production of mRNA by *in vitro* transcription (IVT).[7] While a small set of LOV-T7 RNAP fusion variants resulting from our first approach maintained activity and showed some response to illumination with blue light, we were curious to elucidate the mechanisms of these photoresponses qualitatively and quantitatively, to find additional approaches to identify new and potentially better LOV insertion positions, and to improve the observed effects. In this follow-up study, we employed additional criteria for the identification of insertion sites, generated novel variants, and evaluated the activity and photoresponse of selected (old and new) LOV-T7 RNAP fusion variants using steady-state kinetic experiments and structural modeling techniques.

[a] D. Hafki, J. Alda, D. Pietrus, S. Brakmann
Faculty of Chemistry and Chemical Biology, TU Dortmund University, Otto-Hahn-Str. 4a, Dortmund 44227 Germany
E-mail: susanne.brakmann@tu-dortmund.de

Supporting information for this article is available on the WWW under https://doi.org/10.1002/cbic.202400536

Research Article
doi.org/10.1002/cbic.202400536
Chemistry Europe
European Chemical Societies Publishing

Results and Discussion

Apparent Michaelis-Menten Kkinetics of Photoactive Variants

Series of *in vitro* transcription reactions with or without blue light illumination were performed with three previously identified LOV-T7 RNAP fusion variants (insertion positions with respect to wild-type T7 RNAP: 67/68, 179/180, and 600/601)[5] to study their apparent kinetic parameters K_M and k_{cat} and to gain insight into the structural and mechanistic influences of the inserted LOV domain. For this purpose, we performed IVT with different concentrations of ribonucleoside triphosphates (NTPs) and terminated the reactions at specific times with the RNA-specific fluorophore SYBR Green II, which was also used for the quantitative detection of RNA.[8] The apparent initial velocities v_0 were plotted both directly (Figure 1) and double-reciprocally (Figure 2) and analyzed using the standard Michaelis-Menten equation.

The kinetic data revealed that, despite the domain insertion of 144 amino acids, the maximum velocity of the LOV-T7 RNAP fusion variants in the dark state remained almost identical to that of the wild-type enzyme (Figure 3A and SI, Table S3). Furthermore, it can be concluded that the wild-type enzyme and the studied variants are subject to substrate inhibition at a concentration of $\geq$2 mM NTPs (Figure 1). Irradiation of the LOV variants with light of a wavelength of 470 nm was found to result in a reduction in maximum velocity ($V_{max,app}$) of approximately 30–40% (inhibition or "switch-off" mode). In particular, the light state reaction rates of two of the three variants[3i] (67/68 and 179/180) resulted in a generally flatter curve than that of their dark state reaction. In contrast, the third variant (600/601) exhibited a light state reaction rate that was comparable to that of its dark state over the concentration range from 0.25 mM to approximately 1.25 mM, with a subsequent decline to a $V_{max,app}$ that was approximately 70% of the dark state maximum.

The insertion of the LOV domain into T7 RNAP resulted in changes in the enzyme-substrate interaction. Compared to the wild-type enzyme, the LOV-T7 RNAP fusion variants 66/67 and 179/180 exhibited increased apparent Michaelis-Menten constants ($K_{M,app}$) in the dark state, suggesting that their affinity for the substrates (NTPs) is decreased. In contrast, a decrease in the Michaelis-Menten constant $K_{M,app}$ was observed for variant 600/601, indicating that the interaction with NTPs exhibited by this variant was improved. Under blue light, the $K_{M,app}$ values of all three variants were reduced by approximately 30–50%, thus apparently demonstrating improved enzyme-substrate interaction.

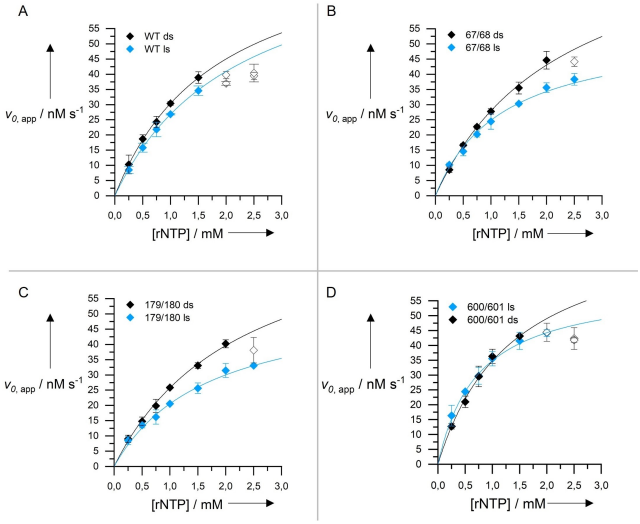

Figure 1. Apparent Michaelis-Menten data for T7 RNAP and LOV-T7-RNAP fusion variants. Data points marked in white were omitted from the curve fitting. Black, dark state (0 lm m^{-2}); blue, light state (92 lm m^{-2}). – A. Wildtype T7 RNAP; B. insertion variant 67/68; C. insertion variant 179/180; D. insertion variant 600/601.

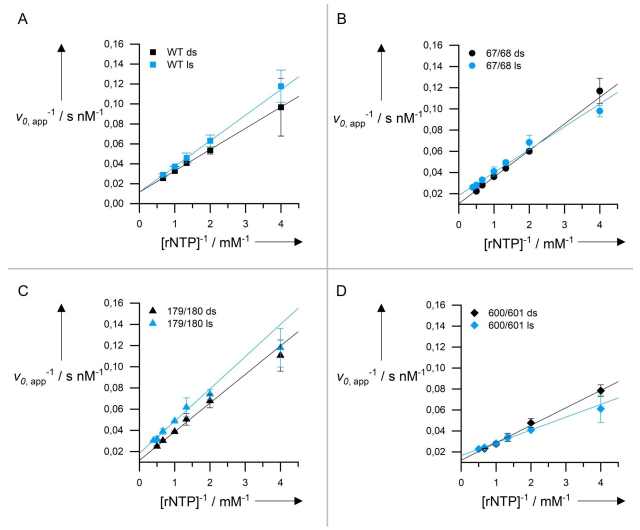

Figure 2. Lineweaver-Burk plots of the apparent Michaelis-Menten data. Black, dark state; blue, light state. – A. Wildtype T7 RNAP; B. insertion variant 67/68; C. insertion variant 179/180; D. insertion variant 600/601.

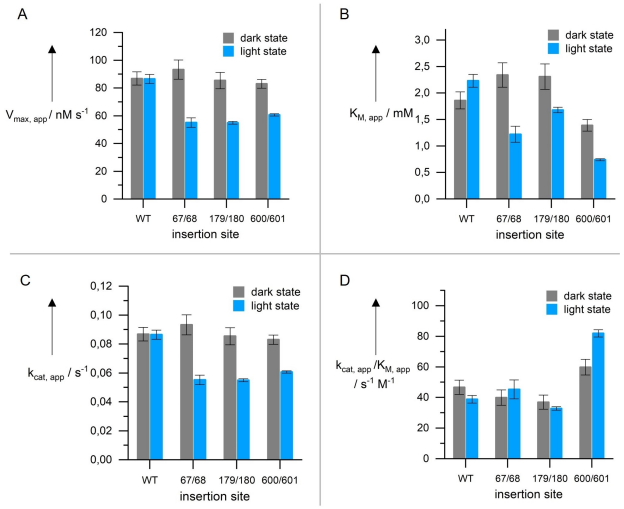

Figure 3. Combined results of apparent Michaelis-Menten kinetics. A. Apparent maximal velocity ($V_{max,app}$); B. apparent $K_{M,app}$; C. apparent turnover number ($k_{cat,app}$); D. apparent catalytic efficiency ($k_{cat,app}/K_{M,app}$).

The k_{cat}/K_M ratios derived from these data indicate that, in particular, the LOV fusion variant 600/601 of T7 RNAP may be of interest for further studies and applications, since the substantial reduction in its $K_{M,app}$ to 50% under illumination, together with a comparatively modest decrease in the maximum velocity $V_{max,app}$ (by about 30 percentage points), almost doubles the catalytic efficiency of this enzyme in the light state compared to wild-type T7 RNAP (Figure 3D).

To classify the type of inhibition exerted on the polymerase by LOV domain insertion, we evaluated the Lineweaver-Burk plots (Figure 2), for which we expected to observe "mixed inhibition" because the LOV domain (assumed to act as an inhibitor) inhibits both the enzyme and the enzyme-substrate complex. The experimental evidence for this type of inhibition is immediately apparent for two variants, 67/68 and 600/601, for which the linear graphs intersect in the first quadrant of the plot. In contrast, the linear graphs for variant 179/180 do not appear to intersect in the same way. This outcome is indicative of an uncompetitive inhibition mechanism, suggesting that steric hindrances or changes to the overall polymerase structure may play an overriding role in this variant.

To correlate the observed effects of these three LOV-T7 RNAP variants with their molecular makeup, we examined their three-dimensional structures after modeling with AlphaFold3.[9]

Structural Analysis Using AlphaFold3

We modeled the structures of LOV-T7-RNAP variants 67/68, 179/180 and 600/601 in both the initiation complex (IC) and elongation complex (EC) using the specific DNA and RNA sequences as in published crystal structure analyses **2pi4**[10] and **1h38**[11] (Figure 4). Using these models, we were able to explain the inhibitory effects observed in our kinetic experiments: All three LOV domain insertions affect one or more of the "tunnels" present in the polymerase structure through which substrates (template DNA, nucleotides) are delivered and products (primarily RNA) are ejected. Obviously, the capacity of the enzyme to carry out catalytic events is reduced when at least one of these tunnels is blocked. Specifically, we observed that in variant 67/68, the inserted LOV domain blocks the RNA exit tunnel (Figure 4A), whereas in variant 179/180, the LOV domain sits "on top" of the polymerase, thereby simultaneously modifying all tunnels (DNA entry, NTP entry, DNA exit, RNA exit; Figure 4B). This adds a general steric hindrance to the "mixed" behavior (i.e., inhibition of the enzyme and the enzyme-substrate complex), resulting in the "uncompetitive" inhibition observed with the kinetic data. The third insertion between residues 600 and 601 shows proximity to the dsDNA entrance tunnel, suggesting that it may form a shape complementary to the DNA major groove and stabilize the contact between the DNA substrate and the enzyme. This could lead to a slowing down of the polymerase action, but also support the binding of NTPs (as evidenced by the lower K_M) and promote catalysis (Figure 4C).

Identification of Novel Insertion Sites

To date, we have obtained and characterized interesting LOV-T7 RNAP variants, but have not been able to achieve either a fully inhibited state or an activated state in response to blue light. Therefore, we investigated whether other insertion sites could be identified by applying different domain insertion criteria that might give us access to better switching properties of LOV-T7 RNAP variants. A number of studies have attempted to identify suitable insertion sites using a variety of approaches. In addition to the split sites that we already used in our previous work,[5] combinatorial libraries[3b,12] or the computational compilation of criteria[13] that must be met by a potential insertion site have been successfully applied. The latter approach requires that the two amino acids between which the LOV domain is to be inserted are not conserved and are located in a solvent-exposed, tight loop between two secondary structural elements.

To implement this strategy for our purposes, we first determined the evolutionary conservation of amino acids within the T7 RNAP primary structure (UniProt: P00573; pdb: **2pi4**[10]) using the MISTIC web server (SI, Figure S1A)[14] starting from a multiple sequence alignment (MSA). According to the published methodology,[13a] all amino acids with a Kullback-Leibler value (also called "relative entropy") below 2 were considered to be

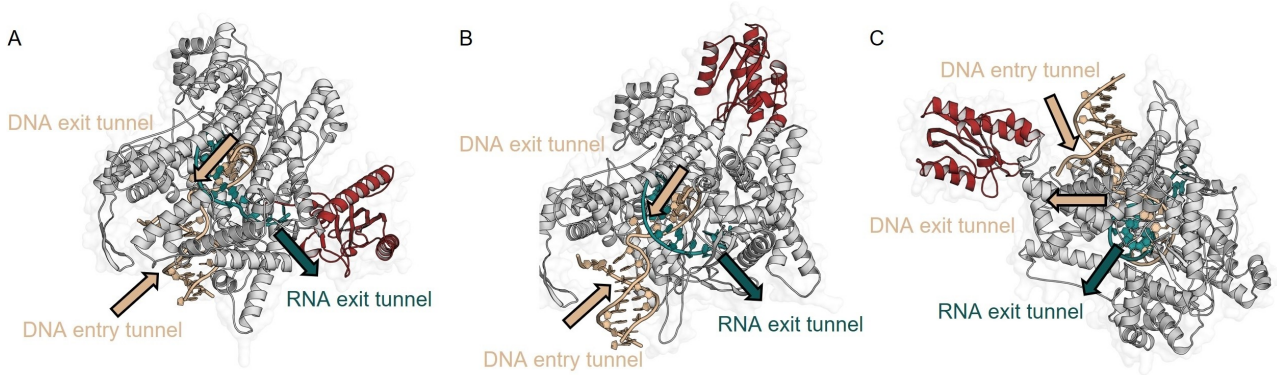

Figure 4. AlphaFold3[9] models of photoactive variants in their elongation complexes. Wheat, dsDNA, teal, RNA, red, AsLOV2. A. Insertion variant 67/68; B. variant 179/180; C. variant 600/601.

evolutionarily nonconserved. In a second step, we used the STRIDE program (SI Figure S1B)[15] to determine the solvent-accessible area (SAA) of all amino acids considering values above 30 Å^2 as solvent-accessible. In the third step, we used the program CMView (SI, Figure S2)[16] to inspect non-conserved and solvent-exposed residues for amino acid contacts in a radius of 7 Å indicating tight loops between secondary structural elements of T7 RNAP. In a final step, potentially suitable insertion sites classified as non-conserved, solvent-exposed loops connecting two secondary structural elements were validated using PyMol[17] resulting in the identification of seven novel insertion sites within T7 RNAP (Figure 5).

Two of these (129/130 and 236/237) were located in the N-terminal domain of the polymerase, while the other sites (470/471, 506/507, 665/666, 713/714, and 730/731) were found within the polymerase domain. In addition to these, we generated another fusion variant (563/564) derived from an insoluble precursor (564/565)[5] by moving the LOV domain insertion site to the center of a loop.

The insertion of the LOV2 coding sequence from *A. sativa* phototropin (NPH1–1; UniProt: O49003, amino acids 404–546; **2v1a**[3d]) into the eight insertion positions identified thus far was carried out using standard cloning procedures. Novel T7 RNAP variants were expressed in *E. coli* and submitted to purification using an established protocol.[5] During purification, two of the eight variants (563/564 and 730/731) became insoluble, while the other six variants were successfully purified (SI, Figure S3).

In Vitro Transcription Reactions

To assess the activity and photoswitchability of the soluble, purified T7 RNAP variants, we performed *in vitro* transcription (IVT) reactions with a double-stranded DNA template (GFP coding sequence under the control of a T7 promoter; approximately 920 bp; SI, Figure S4). Since preliminary experiments showed that IVT reached a steady state already after approximately five minutes, the reactions were terminated after five minutes, either in the absence of light (0 lm m^{-2}) or under illumination with blue light (l = 470 nm, 92 lm m^{-2}). The product RNA was then analyzed on a denaturing agarose gel, stained with ethidium bromide and quantified using ImageJ[18] (SI, Figure S5). However, for some variants, no or only low amounts of RNA were detected after five minutes, so the IVT reactions were repeated with an incubation time of 60 minutes (SI, Figure S6) and analyzed as before. Our experiments revealed that four (out of eight) new LOV-T7 RNAP fusion variants were active, while three of them were also partially inhibited by blue light illumination (Figure 6, SI Table S2).

In contrast to our preliminary experiments, only one new variant, 665/666, produced RNA products within five minutes, while five other variants, 129/130, 236/237, 470/471, 506/507 and 713/714, did not produce any RNA within this time frame. However, three of them, 470/471, 506/507 and 713/714, produced RNA within 60 minutes. Results of IVT under illumination showed that only one of the four active variants, 713/714, showed a clear difference in RNA formation in the light compared to the dark, with a light-induced inhibition of about 30% (SI, Figures S5, S6). In summary, the newly identified insertion sites for a LOV domain did not improve upon the best result for activity and photoresponse obtained in our previous study[5] using "split sites" of T7 RNAP (179/180; 43% inhibition under blue light).

Modification of the Jα Helix

Based on the observation that the distance between the N- and C-terminus of a LOV2 domain becomes more flexible upon irradiation,[3d,e] thereby disrupting neighboring protein folding patterns, we considered a C-terminal extension of the LOV2 Jα helix to increase this distance and the perturbation of T7 RNAP structure and activity. As an example, we used our best variant, 179/180, and extended the C-terminus of its LOV2 domain either with a $(GPP)_2$ motif or with eight or eighteen amino acid residues of a rigid myosin helix (**6obi**[19]). However, none of the resulting protein variants showed any improvement in light-

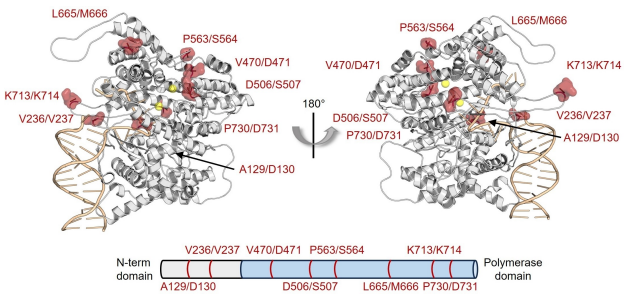

Figure 5. The structure of T7 RNA polymerase in its initiation complex (**2pi4**)[10] with potential insertion sites marked in red. Wheat, dsDNA (T7 promoter); yellow, Mg^{2+} ions.

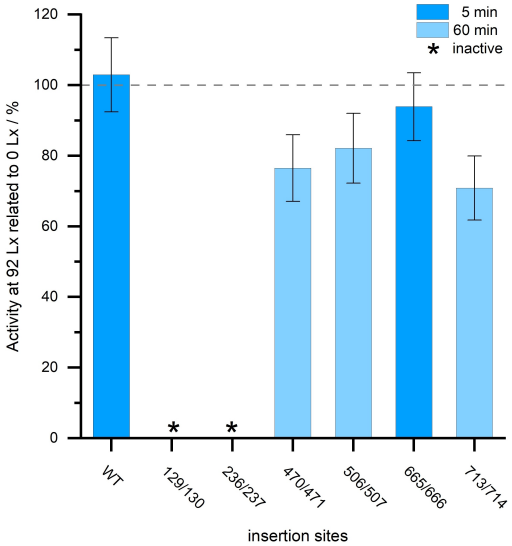

Figure 6. The activities of wild-type T7 RNAP and new LOV insertion variants of T7 RNAP under blue light illumination (470 nm; 92 lm m^{-2}) were related to their activities in the dark (0 lm m^{-2}). Blue, reaction stopped after 5 min; light blue, reaction stopped after 60 min. Numbers indicate the flanking amino acids of an insertion site.

dependent inhibition in IVT reactions that were performed analogously to the experiments described above (Figure 7, SI, Figure S7).

Conclusions

Nucleic acid polymerases such as T7 RNA polymerase, the subject of this study, perform a complex catalytic function that requires the continuous and concerted dynamic interplay of several subdomains. It is therefore remarkable that a representative of this enzyme class is able to tolerate internal fusion ("rewiring") with a photosensory domain while maintaining (most of) its functional and dynamic properties. However, conferring a switching phenotype to T7 RNAP by integral fusion with a LOV2 domain proved to be challenging, as all of the photoresponsive enzyme variants we identified showed a negative modulation (i.e., inhibition) under blue light illumination, which was also only moderate. To date, no variant has been found that was more than approximately 50% inhibited. Approaches for the improvement of these results could be based on the following engineering aspects:

Insertion position. Tolerated insertion sites were found throughout the polymerase protein with no apparent preference for the N-terminal domain or the polymerase domain. Insertion sites selected by computational design were oriented toward loops, as were those derived from split sites. It might be interesting to move these insertion sites to the ends of neighboring helices or β strands, e.g. by mutagenesis, or to search for additional insertion sites by random mutagenesis techniques, e.g. using transposons.

Connecting sequences and linker lengths. From domain insertion experiments, e.g. to create an interdependency of separate protein activities, it is known that the sequences connecting the fusion protein parts play a critical role in the switching behavior and magnitude with shorter linkers promoting switching properties.[12a] For the fusion of LOV2 with T7 RNAP, for example, these sequences could be improved by combinatorial approaches including site-specific mutagenesis to optimize size and polarity or circular permutation and screening or selection to optimize sequences and lengths.[20]

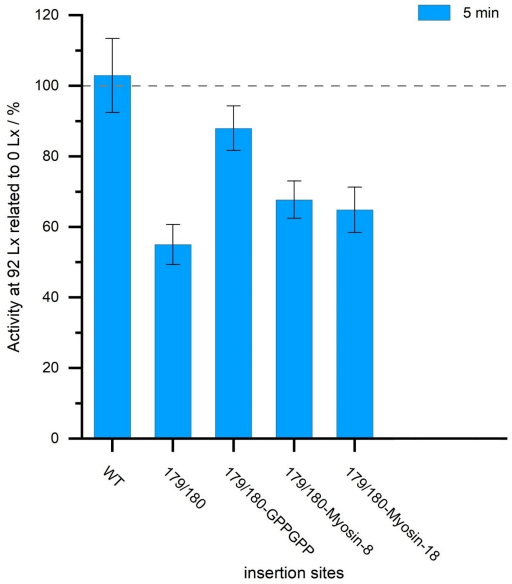

Figure 7. The activities of LOV-T7 RNAP insertion variants with extended Jα helices under blue light illumination (470 nm; 92 lm m^{-2}) were related to their activities in the dark (0 lm m^{-2}).

Light-induced activation vs. inhibition. We have learned from our kinetic experiments and from the modeled 3D structures that the light-induced modulation of LOV-T7 RNAP variants is mainly based on a blockade of substrate entry or product exit tunnels – a phenotype that is more obvious with the presence of an additional domain than the opposite. We conclude that a structural concept for positive modulation would either start from a polymerase in an (auto)-inhibited state or involve a mechanism that influences the enzyme-substrate complex formation by lowering the K_M for DNA or NTPs or both upon blue light illumination. While the former will be more difficult to achieve, the latter could be based on our variant 600/601, which already showed a lower K_M in the dark compared to the wild-type enzyme that was further reduced to 50% upon illumination. (SI, Table S3). As suggested above, adjusting the exact insertion site and the composition and length of the connecting sequences could help address this challenge.

T7 RNAP is a "workhorse" in molecular biology and biotechnology that has been extensively characterized structurally and mechanistically[21] and continues to serve as a prototype for single-subunit (family A) polymerases in a number of structural and functional flexibility studies.[6,22] Because T7 RNAP acts strictly on its cognate promoter, it is functionally orthogonal to common bacterial hosts and can be conveniently studied and applied *in vivo*. A fully and reversibly light-responsive form of this enzyme could be more than just an "upgrade" for biotechnology (e.g., for better control of large-scale protein expression or IVT), but also an important tool for chemical biology (e.g., for perturbing and measuring processes or signaling cascades involving transcription) or synthetic biology (e.g., for designing synthetic gene circuits and information processing structures). In addition, it will be of interest to determine whether the insights gained from our studies of LOV domain insertion can be generalized to other structurally similar polymerases and even to other classes of proteins in order to develop new tools for chemical biology.

Acknowledgements

Open Access funding enabled and organized by Projekt DEAL.

Conflict of Interests

The authors declare no conflict of interest.

Data Availability Statement

The data that support the findings of this study are available from the corresponding author upon reasonable request.

Keywords: Optogenetics · RNA polymerase · Photochemistry · AsLOV2 · Michaelis-Menten kinetics

[1] a) G. Nagel, T. Szellas, W. Huhn, S. Kateriya, N. Adeishvili, P. Berthold, D. Ollig, P. Hegemann, E. Bamberg, *Proc. Natl. Acad. Sci.USA* **2003**, *100*, 13940–13945; b) A. M. Weber, J. Kaiser, T. Ziegler, S. Pilsl, C. Renzl, L. Sixt, G. Pietruschka, S. Moniot, A. Kakoti, M. Juraschitz, S. Schrottke, L. Lledo Bryant, C. Steegborn, R. Bittl, G. Mayer, A. Moglich, *Nat. Chem. Biol.* **2019**, *15*, 1085–1092; c) X. Liao, W. Liu, H. Q. Yang, G. I. Jenkins, *New Phytol.* **2020**, *227*, 857–866; d) A. Dwijayanti, C. Zhang, C. L. Poh, T. Lautier, *Front. Bioeng. Biotechnol.* **2021**, *9*, 804563.

[2] a) A. Baumschlager, S. K. Aoki, M. Khammash, *ACS Synth. Biol.* **2017**, *6*, 2157–2167; b) A. Baumschlager, *Front. Bioeng. Biotechnol.* **2022**, *10*, 901300.

[3] a) S. Seifert, S. Brakmann, *ACS Chem. Biol.* **2018**, *13*, 1914–1920; b) J. Mathony, S. Aschenbrenner, P. Becker, D. Niopek, *Adv. Sci. (Weinh.)* **2023**, *10*, e2303496; c) J. Mathony, D. Niopek, *Adv. Biol. (Weinh.)* **2021**, *5*, e2000181; d) A. S. Halavaty, K. Moffat, *Biochemistry* **2007**, *46*, 14001–14009; e) S. M. Harper, L. C. Neil, K. H. Gardner, *Science* **2003**, *301*, 1541–1544; f) J. N. Iuliano, J. T. Collado, A. A. Gil, P. T. Ravindran, A. Lukacs, S. Shin, H. A. Woroniecka, K. Adamczyk, J. M. Aramini, U. R. Edupuganti, C. R. Hall, G. M. Greetham, I. V. Sazanovich, I. P. Clark, T. Daryaee, J. E. Toettcher, J. B. French, K. H. Gardner, C. L. Simmerling, S. R. Meech, P. J. Tonge, *ACS Chem. Biol.* **2020**, *15*, 2752–2765; g) S. Xiao, M. T. Ibrahim, G. M. Verkhivker, B. D. Zoltowski, P. Tao, *J. Comput. Chem.* **2024**, *45*, 1493–1504; h) P. E. Konold, T. Mathes, J. Weibetaenborn, M. L. Groot, P. Hegemann, J. T. Kennis, *J. Phys. Chem. Lett.* **2016**, *7*, 3472–3476; i) J. Dietler, R. Gelfert, J. Kaiser, V. Borin, C. Renzl, S. Pilsl, A. T. Ranzani, A. Garcia de Fuentes, T. Gleichmann, R. P. Diensthuber, M. Weyand, G. Mayer, I. Schapiro, A. Moglich, *Nat. Commun.* **2022**, *13*, 2618.

[4] F. Takahashi, D. Yamagata, M. Ishikawa, Y. Fukamatsu, Y. Ogura, M. Kasahara, T. Kiyosue, M. Kikuyama, M. Wada, H. Kataoka, *Proc. Natl. Acad. Sci. USA* **2007**, *104*, 19625–19630.

[5] S. Seifert, C. Ehrt, L. Luckfeldt, M. Lubeck, F. Schramm, S. Brakmann, *ChemBioChem* **2019**, *20*, 2813–2817.

[6] a) T. H. Segall-Shapiro, A. J. Meyer, A. D. Ellington, E. D. Sontag, C. A. Voigt, *Mol. Syst. Biol.* **2014**, *10*, 742; b) T. Han, Q. Chen, H. Liu, *ACS Synth. Biol.* **2017**, *6*, 357–366.

[7] a) M. Chamberlin, J. Ring, *J. Biol. Chem.* **1973**, *248*, 2235–2244; b) F. W. Studier, B. A. Moffatt, *J. Mol. Biol.* **1986**, *189*, 113–130; c) A. Dousis, K. Ravichandran, E. M. Hobert, M. J. Moore, A. E. Rabideau, *Nat. Biotechnol.* **2023**, *41*, 560–568.

[8] V. K. Saarnio, K. Salorinne, V. P. Ruokolainen, J. R. Nilsson, T.-R. Tero, S. Oikarinen, L. M. Wilhelmsson, T. M. Lahtinen, V. S. Marjomäki, *Dyes Pigm.* **2020**, *177*, 108282.

[9] J. Abramson, J. Adler, J. Dunger, R. Evans, T. Green, A. Pritzel, O. Ronneberger, L. Willmore, A. J. Ballard, J. Bambrick, S. W. Bodenstein, D. A. Evans, C. C. Hung, M. O'Neill, D. Reiman, K. Tunyasuvunakool, Z. Wu, A. Zemgulyte, E. Arvaniti, C. Beattie, O. Bertolli, A. Bridgland, A. Cherepanov, M. Congreve, A. I. Cowen-Rivers, A. Cowie, M. Figurnov, F. B. Fuchs, H. Gladman, R. Jain, Y. A. Khan, C. M. R. Low, K. Perlin, A. Potapenko, P. Savy, S. Singh, A. Stecula, A. Thillaisundaram, C. Tong, S. Yakneen, E. D. Zhong, M. Zielinski, A. Zidek, V. Bapst, P. Kohli, M. Jaderberg, D. Hassabis, J. M. Jumper, *Nature* **2024**, *630*, 493–500.

[10] W. P. Kennedy, J. R. Momand, Y. W. Yin, *J. Mol. Biol.* **2007**, *370*, 256–268.

[11] T. H. Tahirov, D. Temiakov, M. Anikin, W. T. McAllister, D. Vassylyev, G. S. Yokoyama, *Nature* **2002**, *420*, 43–50.

[12] a) W. R. Edwards, K. Busse, R. K. Allemann, D. D. Jones, *Nucl. Acids Res.* **2008**, *36*, e78; b) W. Coyote-Maestas, Y. He, C. L. Myers, D. Schmidt, *Nat. Commun.* **2019**, *10*, 290.

[13] a) O. Dagliyan, N. V. Dokholyan, K. M. Hahn, *Nat. Protoc.* **2019**, *14*, 1863–1883; b) O. Dagliyan, A. Krokhotin, I. Ozkan-Dagliyan, A. Deiters, C. J. Der, K. M. Hahn, N. V. Dokholyan, *Nat. Commun.* **2018**, *9*, 4042.

[14] F. L. Simonetti, E. Teppa, A. Chernomoretz, M. Nielsen, C. Marino Buslje, *Nucl. Acids Res.* **2013**, *41*, W8–14.

[15] M. Heinig, D. Frishman, *Nucl. Acids Res.* **2004**, *32*, W500–502.

[16] C. Vehlow, H. Stehr, M. Winkelmann, J. M. Duarte, L. Petzold, J. Dinse, M. Lappe, *Bioinformatics* **2011**, *27*, 1573–1574.

[17] Schrödinger, LLC, The PyMOL Molecular Graphics System, Version 2.5.2, **2021**.

[18] C. Schneider, W. Rasband, K. Eliceiri, *Nat. Methods* **2012**, *9*, 671–675.

[19] C. A. Barnes, Y. Shen, J. Ying, Y. Takagi, D. A. Torchia, J. R. Sellers, A. Bax, *J. Am. Chem. Soc.* **2019**, *141*, 9004–9017.

[20] G. Guntas, T. J. Mansell, J. R. Kim, M. Ostermeier, *Proc. Natl. Acad. Sci. USA* **2005**, *102*, 11224–11229.

[21] a) R. Sousa, Y. J. Chung, J. P. Rose, B. C. Wang, *Nature* **1993**, *364*, 593–599; b) D. Jeruzalmi, T. A. Steitz, *EMBO J.* **1998**, *17*, 4101–4113; c) G. M. T. Cheetham, D. Jeruzalmi, T. A. Steitz, *Nature* **1999**, *399*, 80–83; d) T. H. Tahirov, D. Temiakov, M. Anikin, V. Patlan, W. T. McAllister, D. G. Vassylyev, S. Yokoyama, *Nature* **2002**, *420*, 43–50; e) Y. W. Yin, T. A. Steitz, *Cell* **2004**, *116*, 393–404; f) W. P. Kennedy, J. R. Momand, Y. W. Yin, *J. Mol. Biol.* **2007**, *370*, 256–268; g) K. J. Durniak, S. Bailey, T. A. Steitz, *Science* **2008**, *322*, 553–557.

[22] a) J. Lykke-Andersen, J. Christiansen, *Nucl. Acids Res.* **1998**, *26*, 5630–5635; b) J. Huang, L. G. Brieba, R. Sousa, *Biochemistry* **2000**, *39*, 11571–11580; c) V. L. Tunitskaya, S. N. Kochetkov, *Biochemistry (Moskow)* **2002**, *67*, 1124–1135; d) J. Chelliserrykattil, A. D. Ellington, *Nat. Biotechnol.* **2004**, *22*, 1155–1160; e) C. Chou, D. D. Young, A. Deiters, *Chembiochem* **2010**, *11*, 972–977; f) K. M. Esvelt, J. C. Carlson, D. R. Liu, *Nature* **2011**, *472*, 499–503; g) J. Ibach, L. Dietrich, K. R. Koopmans, N. Nobel, M. Skoupi, S. Brakmann, *J. Biotechnol.* **2013**, *167*, 287–295; h) D. L. Shis, M. R. Bennett, *Proc. Natl. Acad. Sci. USA* **2013**, *110*, 5028–5033; i) J. Pu, J. Zinkus-Boltz, B. C. Dickinson, *Nat. Chem. Biol.* **2017**, *13*, 432–438; j) J. Pu, M. Disare, B. C. Dickinson, *Chembiochem* **2019**, *20*, 1547–1553.

Manuscript received: June 20, 2024
Revised manuscript received: August 29, 2024
Accepted manuscript online: September 4, 2024
Version of record online: October 27, 2024